International Journal of Energetica (IJECA)
https://www.ijeca.info
ISSN: 2543-3717 Volume 7. Issue 1. 2022

Mechanical speed estimation of a DFIG based on the Unscented Kalman Filter (UKF)

Hicham Ben Sassi[1], Khadija Lahrech[2], Fatima Errahimi[3], Najia ES-Sbai[3], Mokhtar Ghodbane[4]

[1] *LSEED, Private University of Fez, MOROCCO*
[2] *Laboratory LIPI, National School of Applied Sciences ENSA, USMBA, Fes, MOROCCO*
[3] *Laboratory of Intelligent Systems, Georesources and Renewable Energies (LISGRE). Faculty of Sciences and Technology, Sidi Mohamed Ben Abdellah University. Fez, Box 2202, Fez, MOROCCO*
[4] *Mechanical Engineering Department, Saad Dahlab University of Blida 1, ALGERIA*

[*]Corresponding author E-mail*: ghodbanemokhtar39@yahoo.com*

Abstract – *This work proposes a new estimation technique for the doubly-fed induction generator (DFIG) variables. Researchers have designed numerous sensorless control strategies for the DFIG used either for mechanical speed, electromagnetic torque, or rotor position estimation. In this paper, an analysis of an Unscented Kalman Filter (UKF) will be presented as an observer for both rotor and stator currents, and mechanical speed, which are key information in DFIG control. The performance of the proposed observer has been validated in a 9 MW wind turbine under MATLAB/Simulink. Based on the results obtained, UKF is safely able to replace mechanically coupled sensors which have many disadvantages such as high cost, maintenance, and cabling requirements.*

Keywords*: Sensorless control, Wind energy, DFIG, Observers, Mechanical speed estimation.*

Received: 31/05/2022 – Revised: 20/06/2022 – Accepted: 25/06/2022

I. Introduction

The exploitation of various types of renewable energy sources (solar energy, wind energy, geothermal energy, biomass energy, hydropower) is a particularly viable solution to get rid of dependence on fossil energy sources [1-4]. Regarding wind energy, it has presented itself for the last few years as one of the most reliable and promising renewable energy sources, which can successfully replace fossil energy sources in electricity generation [5-7]. Accordingly, a lot of research activity has been dedicated recently to the problems of control and optimization of renewable energy conversion systems. When it comes to wind energy harvesting, the Doubly-Fed Induction Generator (DFIG) has been widely used in recent years because of its high performance, and its capability to operate under variable wind speeds [8-10]. Furthermore, its rotor power converters are sized to transfer only 30% of the total generated power, which is very eye-catching from a cost-effective point of view [11-13]. However, from a control point of view, the DFIG is still challenging. Many control strategies have been proposed for the DFIG in Wind Energy Conversion System (WECS) such as Stator Voltage Orientation (SVO) and Field Oriented Control (FOC) [14, 15]. The sliding mode control was been presented to overcome the nonlinearity of the system and parameter uncertainties [16, 17]. Backstepping control was also used. However, all of those control strategies require exact knowledge of several DFIG parameters, and variables such as rotor position and speed, electromagnetic flux, and wind speed. Those variables can be obtained by numerous methods such as observers and sensors. Nevertheless, the use of sensors has some drawbacks such as the high cost of cables and sensors and the mechanical coupling problems, as well as the high failure rate, which is due to the use of sensors as tools for data acquisition. As an alternative, the sensorless control of the DFIG using observers is gaining a lot of interest in the last few years [18].

In this regard, several observers have been proposed in

the literature for DFIG parameters estimation, including mechanical speed, rotor position, electromagnetic flux, and wind speed [19-21]. The Model Reference Adaptive System (MRAS) based observer and an MRAS based fuzzy logic technique were used for mechanical speed and rotor position estimation. But because the effectiveness of an MRAS is highly sensitive to the inductance value, recursive techniques like Kalman filters are increasingly being utilized in its place. [22-24]. An Extended Kalman Filter (EKF) was adopted as an observer for the mechanical speed. Nevertheless, this method has some drawbacks including the complexity of the linearization process. As a result, this paper proposes as an alternative observer the Unscented Kalman filter (UKF) to ensure an accurate estimation of the DFIG variables [25, 26].

In this paper, the focus will be on the mechanical speed and both stator and rotor currents because of their significance in the DFIG control. To obtain the values of these parameters an accurate observer is inevitable

II. WECS Modeling

II.1. DFIG Modeling

In the literature, there is no specific and unique model of WECS based on the DFIG as shown in Figure 1 [27], since the model depends on the adopted control strategy. In general, a DFIG based grid-connected WECS consists of a doubly-fed induction generator coupled to the wind turbine through a gear and a shaft. The stator winding of the DFIG is directly connected to the utility grid, and the rotor winding is indirectly connected to the grid through a back-to-back voltage source converter and a transformer. Filters and physical components are also utilized as extra components to control the DFIG during grid faults.

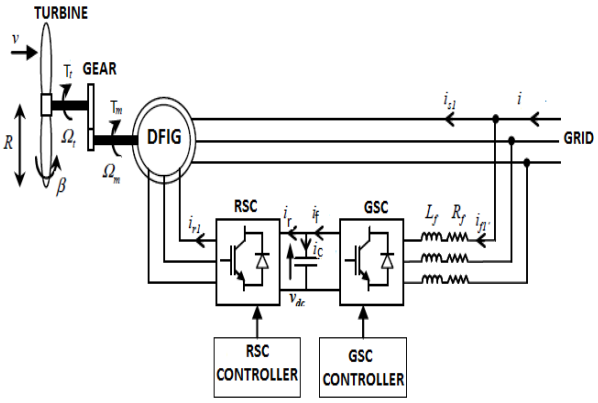

Figure 1. Wind turbine based on the DFIG connected to the grid

Based on the electrical differential equations of both the rotor and the stator, which are converted to direct and quadratic reference with the help of Park transformation, the d-q components of the rotor and the stator voltage equations are expressed in Eq. (1). These currents are expressed as a function of the stator flux linkages (φ_{sd}, φ_{sq}), stator resistance R_s, stator currents (i_{sd}, i_{sq}), stator angular velocity ω_s, rotor flux linkages (φ_{rd}, φ_{rq}), rotor resistance R_r, rotor currents (i_{rd}, i_{rq}), and the slip angular velocity ω_r.

$$\begin{cases} V_{sd} = R_s I_{sd} + \dfrac{d\varphi_{sd}}{dt} - \omega_s \varphi_{sq} \\ V_{sq} = R_s I_{sq} + \dfrac{d\varphi_{sq}}{dt} + \omega_s \varphi_{sd} \\ V_{rd} = R_r I_{rd} + \dfrac{d\varphi_{rd}}{dt} - \omega_r \varphi_{rq} \\ V_{rq} = R_r I_{rq} + \dfrac{d\varphi_{rq}}{dt} + \omega_r \varphi_{rd} \end{cases} \quad (1)$$

$$W_r = W_s - P\Omega_m \quad (2)$$

The equations for the rotor and stator flux linkages are provided in Eq. (3), where M is the mutual inductance and Lr and Ls, respectively, stand in for the rotor and stator self-inductances.

$$\begin{cases} \Phi_{sd} = L_S I_{sd} + M I_{dr} \\ \phi_{sq} = L_S I_{sq} + M I_{qr} \\ \phi_{rd} = L_r I_{rd} + M I_{ds} \\ \phi_{rq} = L_r I_{rq} + M I_{qs} \end{cases} \quad (3)$$

According to the electrical equations of the DFIG, the stator and rotor active and reactive powers are given in Eq. (4).

$$\begin{cases} P_s = \dfrac{3}{2}(V_{ds} I_{sd} + v_{qs} I_{qs}) \\ Q_s = \dfrac{3}{2}(v_{qs} I_{sd} - v_{ds} I_{qs}) \\ P_R = \dfrac{3}{2}(v_{dr} I_{rd} + v_{qr} I_{qr}) \\ Q_R = \dfrac{3}{2}(v_{qr} I_{rd} - v_{dr} I_{qr}) \end{cases} \quad (4)$$

One of the most crucial parameters for mechanical speed estimation is the electromagnetic torque which is expressed in Eq. (5), as a function of the rotor's current, stator flux, and both mutual inductance and stator self-inductances, as well as the number of pair of machine poles.

$$T_{em} = \frac{3}{2} P.M.Ls(\phi_{sq} I_{rd} - \phi_{sd} I_{rq}) \quad (5)$$

II.2. Wind Turbine Model

The turbine represents the organ responsible for transforming the kinetic energy of the wind into a mechanical power given in Eq. (6).

$$P_m = \frac{1}{2}.C(\lambda,\beta).\rho.S.v^3 \quad (6)$$

Where ρ is the air density, $(S = \pi.R^2)$, S is the total area swept by the turbine blades and R is the radius of the blades. $C(\lambda,\beta)$ is the coefficient of power which is the fraction between the kinetic energy of the wind and mechanical power extracted by the turbine. Concerning $C(\lambda,\beta)$ given in Eq. (7), it is a function that depends on the pitch angle (β) and the tip speed ratio (λ) gave by Eq. (8).

$$C(\lambda,\beta) = 0.5872(116A - 0.4\beta - 5)\exp(-21A) + 0.0085\lambda \quad (7)$$

$$\text{with, } A = \frac{1}{\lambda + 0.08\beta} - \frac{0.035}{\beta^3 + 1}$$

$$\lambda = \frac{R\Omega}{v} \quad (8)$$

The basic dynamic equation of the mechanical system provides an explanation for the change of mechanical speed.

$$J_T \frac{d\Omega_{méc}}{dt} + f_v\Omega_{mec} = T_{mec} - T_{em} \quad (9)$$

Where T_{mec} is the mechanical torque, J_T is the moment of inertia, and f is the viscous friction coefficient.

II.3. DFIG State-space model

One of the requirements in the design of the Unscented Kalman Filter is a nonlinear state-space model of the DFIG. Therefore, Based on the basic mechanical system dynamic equation "Eq. (9), , as well as the differential electrical equations of the DFIG previously presented in Eqs. (1-5), a state-space model of the DFIG is given in Eqs. (10) and (11).

$$\frac{dx}{dt} = f(x,u) \quad (10)$$

$$y = h(x) \quad (11)$$

Where x is the stat variable, y is the output (measurement) vector, and u is the input vector.

$$x = (Isd\ Isq\ Ird\ Irq\ wr\ \theta\ Tm)^T \quad (12)$$

$$u = (Vsd\ Vsq\ Vrd\ Vrq) \quad (13)$$

$$y = (Isd\ Isq\ Ird\ Irq) \quad (14)$$

$$f(x,u) = \begin{bmatrix} -\left(\frac{Rs}{\sigma Ls}\right)Isd + \left(\left(\left(\frac{1-\sigma}{\sigma}\right)wr\right) + ws\right)Isq + \left(\frac{Rr.M}{\sigma LsLr}\right)Ird + \left(\frac{M}{\sigma Ls}\right)Wr.Irq + \left(\frac{1}{\sigma Ls}\right)Vsd - \left(\frac{M}{\sigma LsLr}\right)Vrd \\ -\left(\left(\frac{1-\sigma}{\sigma}\right)wr + ws\right)Isd - \left(\frac{Rs}{\sigma Ls}\right)Isq - \left(\frac{M}{\sigma Ls}\right)wr.Ird + \left(Rr.\frac{M}{\sigma LsLr}\right)Irq + \left(\frac{1}{\sigma Ls}\right)Vsq - \left(\frac{M}{\sigma LsLr}\right)Vrq \\ \left(\frac{Rs.M}{\sigma LrLs}\right)Isd - \left(\frac{M}{\sigma Lr}\right)wr.Isq - \left(\frac{Rr}{\sigma Lr}\right)Ird + \left(ws - \frac{wr}{\sigma}\right)Irq - \left(\frac{M}{\sigma LsLr}\right)Vsd + \left(\frac{1}{\sigma Lr}\right)Vrd \\ \left(\frac{M}{\sigma Lr}\right)Isd.wr + \left(Rs.\frac{M}{\sigma LsLr}\right)Isq - \left(ws - \frac{wr}{\sigma}\right)Ird - \left(\frac{Rr}{\sigma Lr}\right)Irq - \left(\frac{M}{\sigma LsLr}\right)Vsq + \left(\frac{1}{\sigma Lr}\right)Vrq \\ \frac{P}{J}.Tm - \frac{3}{2}.P^2.\frac{M}{J}(Isq.Ird - Isd.Irq) - \frac{f}{J}.wr \\ wr \\ 0 \end{bmatrix} \quad (15)$$

Where $\sigma = 1 - \frac{M^2}{Lr.Ls}$.

And

$$h(x) = \begin{bmatrix} 1 & 0 & 0 & 0 & 0 & 0 & 0 \\ 0 & 1 & 0 & 0 & 0 & 0 & 0 \\ 0 & 0 & 1 & 0 & 0 & 0 & 0 \\ 0 & 0 & 0 & 1 & 0 & 0 & 0 \\ 0 & 0 & 0 & 0 & 0 & 0 & 0 \\ 0 & 0 & 0 & 0 & 0 & 0 & 0 \\ 0 & 0 & 0 & 0 & 0 & 0 & 0 \end{bmatrix}.x \quad (16)$$

III. Unscented Kalman Filter

III.1. Unscented Transformation

Kalman Filters are one of the most powerful algorithms for solving estimation problems. Accordingly, an Unscented Kalman Filter (UKF) has been adopted in this work. The Unscented Transformation (UT) of non-linear systems serves as the foundation for the UKF. In order to deal with any nonlinearity in the system, this novel approach is based on computing the statistic mean

and covariance of a random variable that goes through the nonlinear transformation Y=f(x). Figure 2 depicts the technique's working principal.

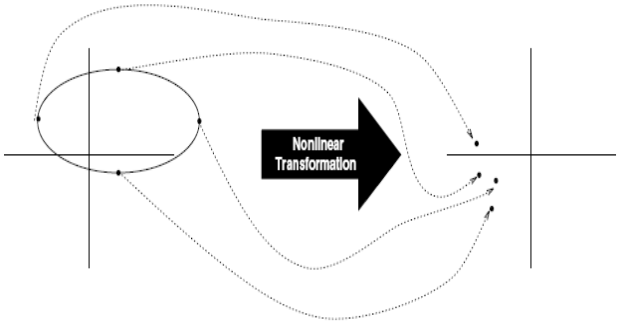

Figure 2. Unscented Transformation (UT)

The UT procedure:

- *Compute a set of Sigma points*

$$\begin{aligned} \tilde{X}0 &= \overline{X}(k-1) \\ \tilde{X}^{(i)}(k-1) &= \overline{X}(k-1) \\ &\quad + \left(\sqrt{(n+\lambda)P_k}\right) i, \text{for } i \\ &\quad = 1,2,\dots,n \end{aligned} \tag{17}$$

$$\begin{aligned} \tilde{X}^{(i)}(k-1) &= \\ \overline{X}(k-1) - \left(\sqrt{(n+\lambda)P_k}\right) &i, \text{for } i = n+ \\ 1,\dots,2n & \end{aligned}$$

λ is the scaling parameter.

$$\lambda = \alpha^2(n+K) - n \tag{18}$$

While (α) defines the range of sigma points surrounding the mean X value. In most cases, has a value between 0 and 1 ([0,1]) [26]. The system's dimension is represented by n. The second scaling factor, k, is frequently set to K=3-n. P_K and $\overline{X}$ are the covariance matrix and X's mean, respectively. The weight assigned to each sigma point is as follows:

$$\begin{aligned} Wm^{(0)} &= {}^{\lambda}/_{(n+\lambda)} \\ Wc^{(0)} &= Wm^{(0)} + (1-\alpha^2+\beta) \\ Wm^{(i)} &= Wc^{(i)} = {}^{\lambda}/_{[2.(n+\lambda)]} \end{aligned} \tag{19}$$

As a constraint, the weights must sum up to 1.

$$\sum_{i=0}^{2n} W^i = 1 \text{ , for } i = 1.2 \dots 2n \tag{20}$$

Where β is an additional scaling parameter that takes into account knowledge about the distribution of X from the past. The best option in the case of a Gaussian distribution is β =2. The terms mean and covariance are denoted by the symbols (m) and (c).

- *Use the nonlinear function to propagate each sigma point and produce a series of altered samples.*

$$Y^i = f(X^i) \text{ , for } i = 1.2 \dots 2n \tag{21}$$

- *Utilizing the weighted mean $\bar{Y}$ and covariance of the prior samples, compute the mean Y and covariance matrix for Y.*

$$\bar{Y} = \sum_{i=0}^{2n} Wm^i . Y^i \text{ , for } i = 1,2,\dots,2n \tag{22}$$

$$\begin{aligned} P_k = \sum_{i=0}^{2n} Wc^i . (Y^i - \bar{Y})(Y^i - \bar{Y})^T \text{ , for } i \\ = 1,2,\dots,2n \end{aligned} \tag{23}$$

III.2. The Unscented Kalman filter

In this section, an Unscented Kalman Filter (UKF) is adopted for estimating DFIG system variables, given that the adopted UKF is a derivative-free filtering algorithm.

Therefore, as shown in references [26-29], the UKF algorithm for background theory is presented as follows:

- *Step 1. Initialization*

$$\begin{aligned} Q(k) &= E\{w_k {w^T}_k\}; \\ R(k) &= E\{v_k {v^T}_k\}\,; E\{w_k {v^T}_k\} = 0 \end{aligned} \tag{24}$$

$$P_0 = E[(x_0 - \bar{x}_0)(x_0 - \bar{x}_0)^T] \tag{25}$$

$$\bar{X}_0 = E[x_0] \tag{26}$$

Where Q(k) and R(k) are diagonal matrices that represent respectively the process noise covariance and the observation noise covariance.

- *Step 2. Compute Sigma points*

From Eq. (17), sigma points can be calculated.

$$\begin{aligned} \mathcal{X}_{k-1} &= [\bar{x}_{k-1}, \\ \bar{x}_{k-1} + \left(\sqrt{(n+\lambda)P^-_{x,k-1}}\right) &, \bar{x}_{k|k-1} - \\ \left(\sqrt{(n+\lambda)P^-_{x,k-1}}\right)&] \end{aligned} \tag{27}$$

- *Step 3. Prediction phase*

The propagation of the sigma points through the system/state equation is given by:

$$\mathcal{X}^{(i)}_{k|k-1} = f(\mathcal{X}^{(i)}_{k-1}, ik) \tag{28}$$

The following is a formula for calculating propagated mean and covariance:

$$\bar{x}_{k|k-1} = \sum_{i=0}^{2n} Wm . \mathcal{X}^{(i)}_{k|k-1} \tag{29}$$

$$P^{-}_{x,k|k-1} = \sum_{i=0}^{2n} Wc[\mathcal{X}^{(i)}_{k|k-1} - \bar{x}_{k|k-1}][\mathcal{X}^{(i)}_{k|k-1} - \bar{x}_{k|k-1}]^{T} + Q_{k-1} \quad (30)$$

The new sigma points matrix using is given by:

$$\bar{x}_{k|k-1} \text{ and } P^{-}_{x,k|k-1}.$$
$$\mathfrak{x}_{k|k-1} = \left[\bar{x}_{k|k-1}, \bar{x}_{k|k-1} + \left(\sqrt{(n+\lambda)P^{-}_{x,k|k-1}}\right), \bar{x}_{k|k-1} - \left(\sqrt{(n+\lambda)P^{-}_{x,k|k-1}}\right)\right] \quad (31)$$

The propagation of the new sigma point through the nonlinear function is given by:

$$y^{(i)}_{k|k-1} = H(\mathfrak{x}^{(i)}_{k|k-1}, ik) \quad (32)$$

a) Calculate the mean of the output variable.

$$\bar{y}_{k|k-1} = \sum_{i=0}^{2n} Wm.\, y^{(i)}_{k|k-1}, \text{ for i=1,…,2n} \quad (33)$$

- *Step 4. Measurement update*

The covariance between the measurement vector and the cross-covariance is calculated as:

$$P_{y.k} = \sum_{i=0}^{2n} Wc[y^{(i)}_{k|k-1} - \bar{y}_{k|k-1}][y^{(i)}_{k|k-1} - \bar{y}_{k|k-1}]^{T} \quad (34)$$

$$P_{xy.k} = \sum_{i=0}^{2n} Wc[\mathfrak{x}^{(i)}_{k|k-1} - \bar{x}_{k|k-1}][y^{(i)}_{k|k-1} - \bar{y}_{k|k-1}]^{T} \quad (35)$$

Kalman gain is given by:

$$K_k = P_{xy.k}.P^{-1}_{y.k} \quad (36)$$

The state estimate update and the covariance estimate update are presented as follows:

$$\hat{X}_k = \hat{X}_{k|k-1} + K_k(y_k - \bar{y}_{k|k-1}) \quad (37)$$

$$\hat{P}_k = P^{-}_{x.k|k-1.} - K.P_{y.k}.K^{T} \quad (38)$$

IV. Results and Discussion

Simulation and tests were conducted to verify the robustness of the proposed observer for parameter estimation relying on a 9 MW model of WTS based on DFIG implemented in MATLAB/Simulink. The WTS parameters used for simulations are given in Table 1.

Table 1. Parameters used in the simulation

Name	Symbol	Value
DFIG rated power (base power)	P_{nom}	9Mw
Stator voltage (base voltage)	$U_{nom\ stator}$	400V
Rotor voltage (base voltage)	$U_{nom\ rotor}$	1975V
Grid frequency	f_0	50Hz
Number of pair poles	P	3
Stator resistance	R_s	0.023(Pu)
Rotor resistance	R_r	0.016(Pu)
Stator inductance	L_s	0.18(Pu)
Rotor inductance	L_r	0.16(Pu)
Mutual inductance	M	2.9(Pu)

Figures 3 to 6 exhibit the measured and estimated stator and rotor currents, respectively. The simulation results reveal that the proposed observer UKF works very well in estimating the stator and rotor currents.

The simulation results shown in Figure 3 show that the UKF performs the estimation of direct and quadratic stator currents. Based on these results, it is clear that the tracking performance and convergence velocity of UKF are satisfactory regardless of the rapid differences in currents observed at the start of the simulation. Moreover, the rated stator currents given in red are almost identical to the real currents given in red with a maximum error of 1%, which displays the accuracy of the UKF.

The results of Figures 4 and 5 also show the estimation for the direct and quadratic components of the rotor current. Similar to the case of the stator, the rated rotating currents given in blue converge instantly towards the real currents given in red, further illustrating the efficiency of the UKF.

Figure 6 shows the dynamic response and tracking performance of the UKF for the DFIG mechanical velocity estimation, where it is clear that the rated velocity given in red was able to follow the measured velocity with great accuracy of max 1.3%. This confirms and verifies the robustness of the proposed controller and its ability to replace the mechanically coupled sensor.

As shown in Figures (3-6), the estimated currents converge towards the measured currents instantly and with great accuracy. This reflects the convergence speed of the observer as well as its accuracy.

Furthermore, based on the results presented in Figure 7, it is clear that the estimated velocity of the rotor follows with great accuracy the measured velocity, which

confirms and verifies the robustness of the proposed observer, and its capability to replace the mechanically coupled sensor.

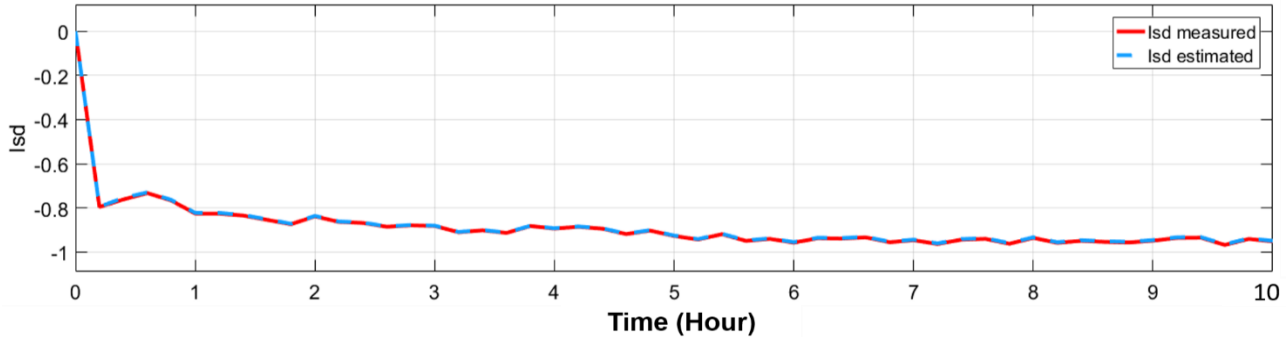

Figure 3. Estimated and real currents of DFIG stator

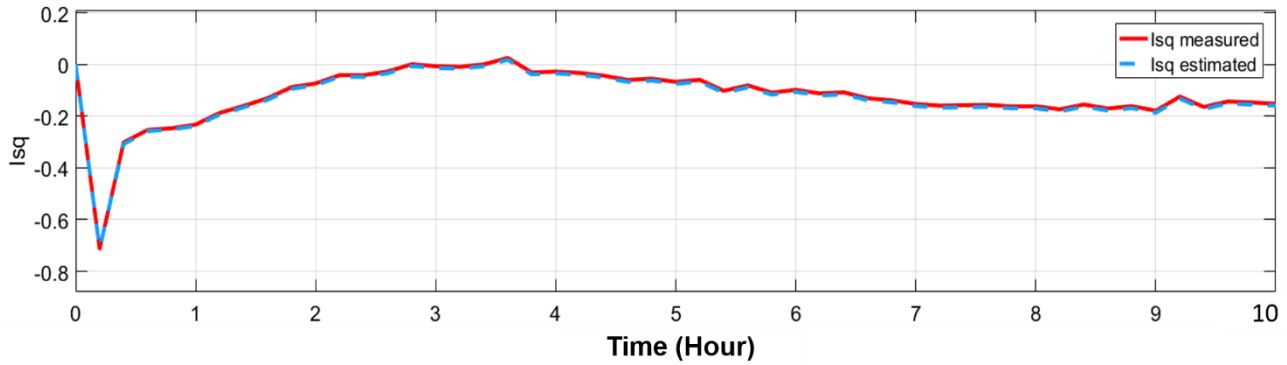

Figure 4. Estimated and real quadratic currents of DFIG stator

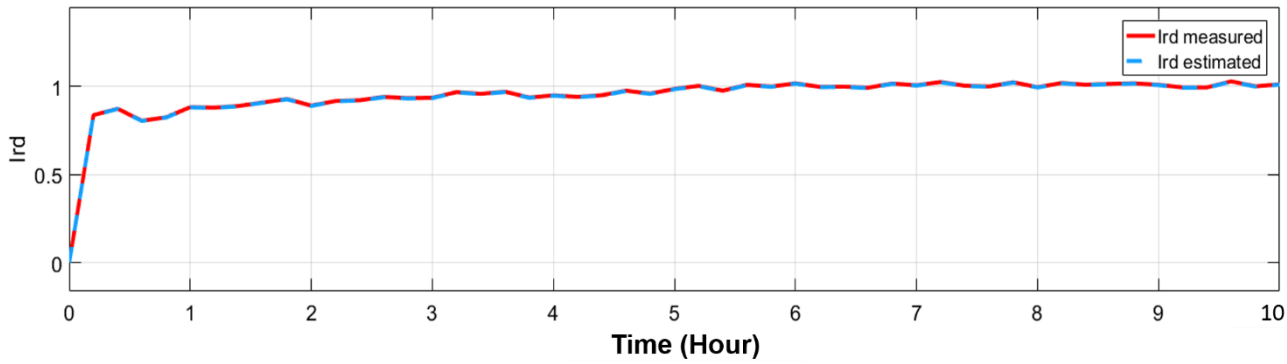

Figure 5. Estimated and real direct current of the DFIG rotor

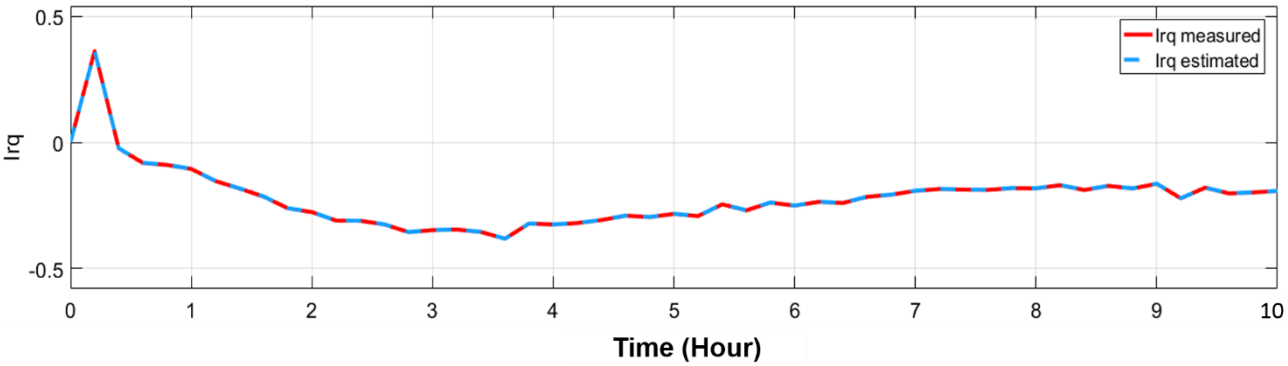

Figure 6. The estimated and real quadratic current of the DFIG rotor.

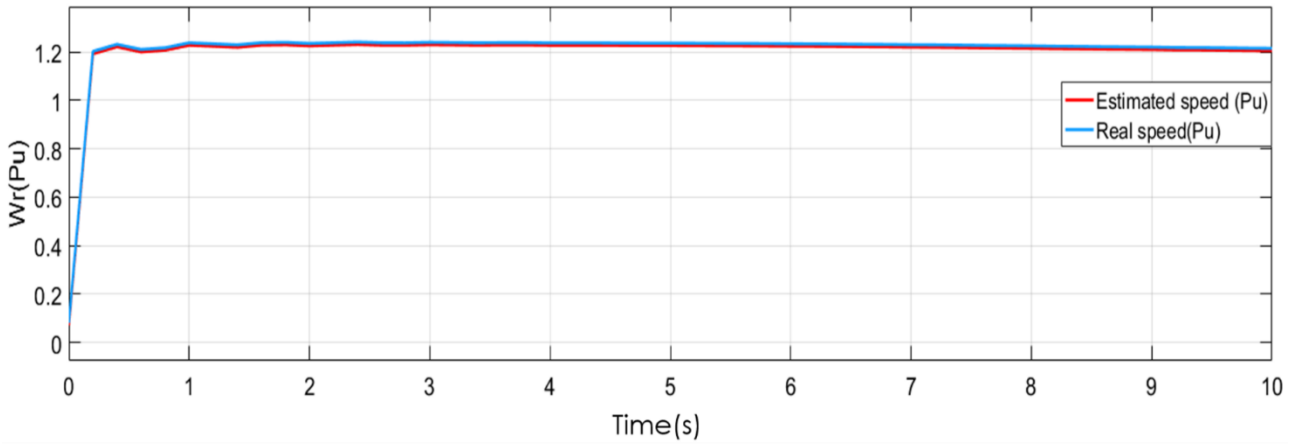

Figure 7. Real and estimated speed of the rotor

Since the performance of the observer is measured based on the speed and accuracy of convergence, in this section the efficiency of the UKF has been compared with other strategies adopted in the literature for estimating the mechanical velocity of DFIG. This includes the High-Order Sliding Mode Observer (HOSMO), which has been studied in study [30]. Although HOSMO was able to get close to its true rotor speed, it suffers from a collapsing phenomenon that affects the accuracy of the results. Moreover, the convergence velocity of HOSMO is relatively slow 0.5 seconds compared to that of the UKF which was almost instantaneous. In another study, compared to the MRAS monitor examined in the study [22], the UKF is also superior in terms of convergence velocity, with the authors stating that MRAS converges after 18 seconds, while in this paper the UKF took less than 0.1 seconds. For rotor velocity estimation, a second-order generalized integrator is used; however, because the system needs two synchronization cycles, as stated by the authors [31], its convergence velocity is slower than that of the UKF.

Based on the above results, it can be asserted that UKF is safely able to replace the mechanically coupled sensor as it suffers from several disadvantages including high cost and maintenance, and cabling requirements [32]. Furthermore, since the UKF was able to accurately estimate both the direct and quadratic components of the stator and rotor currents, it is possible to rely only on these rated currents rather than the measured currents to control the active and reactive forces of the stator and rotor using Eq. (4), as this can help overcome the added noise of existing sensors during power calculation and control.

V. Conclusion

Since wind energy has emerged as one of the most dependable and promising renewable energy sources, there has been a lot of interest in trying to improve the efficiency of its conversion systems recently. In this regard, this paper investigated the performances of an Unscented Kalman filter which is proposed as an alternative for mechanical sensors in speed measurement, whereas, simulations and tests were carried out to verify the robustness of the proposed observer for parameter estimation based on the 9MW model of WTS based on DFIG applied in MATLAB/Simulink. The obtained results have shown that the UKF was able to track the rotor's speed with high accuracy and impressive convergence time, which confirms the robustness of the UKF and its suitability for such tasks. Therefore, UKF is safely able to replace mechanically coupled sensors which have many disadvantages such as high cost, maintenance, and cabling requirements.

Declaration

- The authors declare that they have no known financial or non-financial competing interests in any material discussed in this paper.
- The authors declare that this article has not been published before and is not in the process of being published in any other journal.
- The authors confirmed that the paper was free of plagiarism.

References

[1] Z. Said, M. Ghodbane, B. Boumeddane, A.K. Tiwari, L.S. Sundar, C. Li, N. Aslfattahi, E. Bellos, "Energy, exergy, economic and environmental (4E) analysis of a parabolic trough solar collector using MXene based silicone oil nanofluids," Solar Energy Materials and Solar Cells, vol. 239, 111633. 2022. https://doi.org/10.1016/j.solmat.2022.111633

[2] Z. Said, P. Sharma, N. Aslfattahi, M. Ghodbane, "Experimental analysis of novel ionic liquid-MXene hybrid nanofluid's energy storage properties: Model-prediction using modern ensemble machine learning methods," Journal of Energy Storage, vol. 52, 104858. 2022. https://doi.org/104810.101016/j.est.102022.104858

[3] M. Ghodbane, Z. Said, A.K. Tiwari, L. Syam Sundar, C. Li, B. Boumeddane, "4E (energy, exergy, economic and environmental) investigation of LFR using MXene based silicone oil nanofluids," Sustainable Energy Technologies and Assessments, vol. 49, 101715. 2022. https://doi.org/10.1016/j.seta.2021.101715

[4] M. Ghodbane, Boumeddane, K. Lahrech, "Solar thermal energy to drive ejector HVAC systems: A numerical study under Blida climatic conditions," Case Studies in Thermal Engineering, vol. 28, 101558. 2021. https://doi.org/10.1016/j.csite.2021.101558

[5] E. Douvi, D. Douvi, D. Pylarinos, D. Margaris, "Effect of Rain on the Aerodynamic Performance of a Horizontal Axis Wind Turbine – A Computational Study," International Journal of Energetica, vol. 6, pp. 25-33. 2021. https://dx.doi.org/10.47238/ijeca.v6i1.158

[6] Y. Saidi, A. Mezouar, Y. Miloud, M. A. Benmahdjoub, M. Yahiaoui, "Fuzzy Logic Based Robust DVC Design of PWM Rectifier Connected to a PMSG WECS under wind/load Disturbance Conditions," International Journal of Energetica, vol. 4, pp. 37-43. 2019. https://dx.doi.org/10.47238/ijeca.v4i1.84

[7] H. Cherif, A. Khechekhouche, M. Maamir, H. Aboub, B. Belgasim, "Modelling and Control of a Small Domestic Wind Turbine," ASEAN Journal of Science and Engineering, vol. 3, pp. 115-122. 2023. https://doi.org/10.17509/ajse.v3i1.44725

[8] H. Mesai Ahmed, A. Bentaallah, Y. Djeriri, A. Mahmoudi, "Comparative study between pi and fuzzy pi controllers for DFIG integrated in variable speed wind turbine," International Journal of Energetica, vol. 4, pp. 8-13. 2019. https://dx.doi.org/10.47238/ijeca.v4i2.102

[9] G. Nurettin, A. Sevinç, "Performance study and analysis between vector control and direct power control for DFIG based wind energy system," International Journal of Energetica, vol. 6, pp. 13-20. 2021. https://dx.doi.org/10.47238/ijeca.v6i2.175

[10] M. Atallah, A. Mezouar, Kh. Belgacem, Y. Saidi, M. A. Benmahdjoub, "Modeling and Power Control of 5th and 3rd order model for DFIG Applied of Wind Conversion System," International Journal of Energetica, vol. 6, pp. 44-51. 2021. https://dx.doi.org/10.47238/ijeca.v6i2.170

[11] Ashwani Kumar, Sanjay K. Jain, "A Review on the Operation of Grid Integrated Doubly Fed Induction Generator," International Journal of Enhanced Research in Science Technology & Engineering, vol. 2, pp. 25-37. 2013

[12] A. Petersson. Analysis, "Modeling and Control of Doubly-Fed Induction Generators for Wind Turbines," PhD Thesis, Chalmers University of Technology. 2005

[13] G. Salloum, "Contribution à la commande robuste de lamachine asynchrone a double alimentation," PhD Thesis, l'institut national polytechnique de Toulouse. 2007

[14] C. Batlle, A D`oria-Cerezo, R. Ortega, "A Stator Voltage Oriented PI Controller For The Doubly-Fed Induction Machine," Proceedings of the 2007 American Control Conference Marriott Marquis, New York City, USA, July 11-13, 2007

[15] B. Bossoufi, H. A. Aroussi, E. M. Ziani, A. Lagrioui, A. Derouich, "Low-Speed Sensorless Control of DFIG Generators Drive for Wind Turbines System," WSEAS transactions on systems and control, vol. 4, pp. 514-525. 2014

[16] S. Kouadria, Y Messlem, E. Berkouk, "Sliding mode control of active and reactive power of DFIG for variable-speed wind energy conversion system," Proceedings of the 3rd International Renewable and Sustainable Energy Conference (IRSEC), Marrakech – Ouarzazate, Morocco, December 10-13, 2015

[17] S. Ebrahimkhani, "Robust fractional order sliding mode control of doubly-fed induction generator (DFIG)-based wind turbines," ISA Transactions, vol. 63, pp. 343-354. 2016

[18] M. El Azzaoui, H. Mahmoudi, C. Ed-dahmani, "Backstepping control of a doubly fed induction generator integrated to wind power system," 2nd International Conference on Electrical and Information Technologies, Tangier, Morocco, pp. 306-311. 2016

[19] M. Abdelrahem, C. Hackl and R. Kennel, "Application of extended Kalman filter to parameter estimation of doubly-fed induction generators in variable-speed wind turbine systems," International Conference on Clean Electrical Power (ICCEP), pp. 226-233. 2015. https://doi.org/10.1109/ICCEP.2015.7177628

[20] B. Singh and N. K. S. Naidu, "Direct power control of single VSC based DFIG without rotor position sensor," IEEE International Conference on Power Electronics, Drives and Energy Systems (PEDES), pp. 1-6. 2012. https://doi.org/10.1109/PEDES.2012.6484384

[21] Y. Majdoub, A. Abbou, M. Akherraz, "Variable Speed Control of DFIG-Wind Turbine with Wind Estimation," International Renewable and Sustainable Energy Conference (IRSEC), pp. 268-274. 2014. https://doi.org/10.1109/IRSEC.2014.7059879

[22] R. Cardenas, R. Pena, J. Proboste, G. Asher, J. Clare, "MRAS observer for sensorless control of standalone doubly fed induction generators," in IEEE Transactions on Energy Conversion, vol. 20, pp. 710-718. 2005. https://doi.org/10.1109/TEC.2005.847965

[23] A. Mehdi, A. Reama, H. Benalla, "MRAS observer for sensorless direct active and reactive power control of DFIG based WECS with constant switching frequency," Eleventh International Conference on Ecological Vehicles and Renewable Energies (EVER), pp. 1-7. 2016. https://doi.org/10.1109/EVER.2016.7476349

[24] K. Belmokhtar, M.L. Doumbia, K. Agbossou, "Novel fuzzy logic based sensorless maximum power point

tracking strategy for wind turbine systems driven DFIG (doubly-fed induction generator)," Energy, vol. 76, pp. 679-693. 2014. https://doi.org/10.1016/j.energy.2014.08.066

[25] M. Abdelrahem, C. Hackl, R. Kennel, "Sensorless Control of Doubly-Fed Induction Generators in Variable-Speed Wind Turbine Systems," International Conference on Clean Electrical Power (ICCEP), pp. 406-413. 2015. https://doi.org/10.1109/ICCEP.2015.7177656

[26] S. J. Julier Jeffrey K. Uhlmann, "A New Extension of the Kalman Filter to Nonlinear Systems," The Robotics Research Group, Department of Engineering Science, The University of Oxford, proceedings of the IEEE, vol. 92. 2004

[27] S. Kumar Senapati, "Modelling and Simulation of a Grid Connected Doubly Fed Induction Generator for Wind Energy Conversion System," Thesis for the degree of Master department of electrical engineering national institute of technology Rourkela, May 2014

[28] Y. Wu, D. Hu, M. Wu, X. Hu, "Unscented Kalman filtering for additive noise case: augmented versus nonaugmented," in IEEE Signal Processing Letters, vol. 12, pp. 357-360. 2005. https://doi.org/10.1109/LSP.2005.845592

[29] B. Huang, Q. Wang, "Overview of emerging Bayesian approach to nonlinear system identification. In Round Tables on Non-linear Model Identification," International Workshop on Solving Industrial Control and Optimization Problems, Cramado, Brazil, April 6–7, 2006

[30] M. Benbouzid, B. Beltran, H. Mangel, A. Mamoune, "A high-order sliding mode observer for sensorless control of DFIG-based wind turbines," IECON Proc. Industrial Electron. Conf., pp. 4288–4292. 2012. https://doi.org/10.1109/IECON.2012.6389200

[31] A. T. Nguyen, D. C. Lee, "Sensorless Control of DFIG Wind Turbine Systems Based on SOGI and Rotor Position Correction," IEEE Trans. Power Electron., vol. 36, pp. 5486–5495. 2021. https://doi.org/10.1109/TPEL.2020.3027888

[32] M. Pucci, M. Cirrincione, "Neural MPPT control of wind generators with induction machines without speed sensors," IEEE Trans. Ind. Electron., vol. 58, pp. 37–47. 2011. https://doi.org/10.1109/TIE.2010.2043043